The Canadian Mineralogist
Vol. 33, pp. 1047-1057 (1995)

SILVER-BEARING SULFOSALTS FROM THE METAMORPHOSED RAMPURA AGUCHA Zn–Pb–(Ag) DEPOSIT, RAJASTHAN, INDIA

WOLFRAM HÖLLER

Institut für Geowissenschaften, Montanuniversität Leoben, Peter-Tunner-Straße 5, 8700 Leoben, Austria

SUBBARAJU MOHANDAS GANDHI

Hindustan Zinc Limited, Yashad Bhavan, 313001 Udaipur, India

ABSTRACT

The sediment-hosted Rampura Agucha Zn–Pb–(Ag) deposit in Rajasthan, India, contains assemblages rich in Ag–(Pb)–Sb sulfosalts. Freibergite $Ag_{3.3-7.6}Cu_{6.5-2.2}Fe_{1.5-3.1}Zn_{0-0.8}Sb_{3.7-4.6}As_{0-0.4}S_{13}$, pyrargyrite, stephanite, argentite, dyscrasite and various Pb–Ag–Sb sulfosalts occur either within or close to large aggregates of galena. Freibergite, pyrargyrite and stephanite also occur in galena-bearing veinlets in silicate minerals. Electron-microprobe analyses reveal an average Ag-content of 31 wt.% in freibergite, whereas galena is devoid of Ag. The sulfosalts are Sb-rich end members of the respective solid-solution series, with only limited As. The assemblages were affected by recrystallization and re-equilibration during high-grade metamorphism and the subsequent cooling. The pyrargyrite presumably formed by replacement of freibergite and of Pb–Ag–Sb sulfosalts, the stephanite, by decomposition of pyrargyrite and argentite, and the dyscrasite, by exsolution from galena.

Keywords: freibergite, pyrargyrite, stephanite, dyscrasite, argentite, boulangerite, Pb–Ag–Sb sulfosalts, metamorphism, Rampura Agucha, Rajasthan, India.

SOMMAIRE

Le gisement à Zn–Pb–(Ag) de Rampura Agucha, au Rajasthan, en Inde, situé dans un encaissant métasédimentaire, contient des assemblages riches en sulfosels à Ag–(Pb)–Sb. On trouve freibergite $Ag_{3.3-7.6}Cu_{6.5-2.2}Fe_{1.5-3.1}Zn_{0-0.8}Sb_{3.7-4.6}As_{0-0.4}S_{13}$, pyrargyrite, stéphanite, argentite, dyscrasite et autres sulfosels à Pb–Ag–Sb dans des amas importants de galène, ou près de ceux-ci. Freibergite, pyrargyrite et stéphanite se trouvent aussi dans des veinules de galène dans des minéraux silicatés. Les analyses à la microsonde électronique révèlent une teneur moyenne en Ag de 31% (poids) dans la freibergite, tandis que la galène ne contient aucun Ag. Les sulfosels sont les termes à Sb des solutions solides respectives, avec très peu d'arsenic. Les assemblages ont été affectés par une recristallisation et un ré-équilibrage au cours d'un épisode de métamorphisme intense et d'un refroidissement par la suite. La pyrargyrite se serait formée par remplacement de la freibergite et des sulfosels à Pb–Ag–Sb, la stéphanite, par déstabilisation de la pyrargyrite et de l'argentite, et la dyscrasite, par exsolution dans la galène.

(Traduit par la Rédaction)

Mots-clés: freibergite, pyrargyrite, stéphanite, dyscrasite, argentite, boulangerite, sulfosels à Pb–Ag–Sb, métamorphisme, Rampura Agucha, Rajasthan, Inde.

INTRODUCTION

Rampura Agucha is a stratiform, sediment-hosted Zn–Pb–(Ag) deposit located some 220 km southwest of Jaipur in Rajasthan State, India (Fig. 1). Since its discovery in 1977, Rampura Agucha has become one of the most significant base-metal deposits in India, producing 900,000 t/a of ore. The proven reserves are 39.2 Mt, probable reserves 13.8 Mt, and possible reserves 10.7 Mt (total 63.7 Mt), grading 13.6% Zn, 1.9% Pb, 9.58% Fe and 45 ppm Ag (HZL Staff 1992). The deposit occurs in the oldest part of the Bhilwara Supergroup, at the contact with the Archean basement ("Banded Gneissic Complex", BGC). The Bhilwara Supergroup, consisting of a pile of metasedimentary rocks intruded by igneous rocks, developed as a result of intracratonic rifting of the Archean basement about 2.0 Ga ago. The deposit was formed by convective circulation of seawater in zones of crustal extension during incipient rifting (Deb 1992). The metals, derived from the hydrothermal system, were accumulated in a trough with biological activity, as indicated

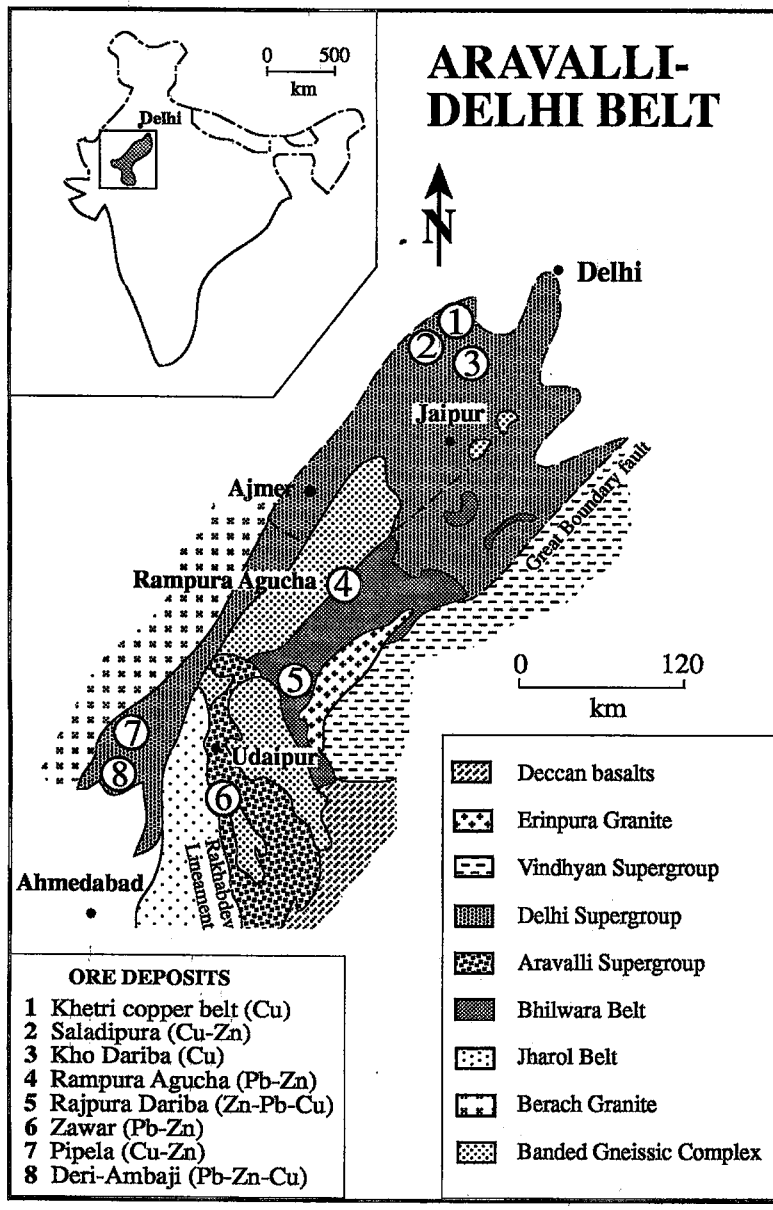

FIG. 1. Simplified geological map of the Delhi-Aravalli belt (after Sugden *et al.* 1990), including the location of the main ore deposits.

by high contents of graphite and light $\delta^{13}C$ values (Deb 1992, Deb & Sarkar 1990). This suggests a relatively deep-water, reducing environment during sedimentation, in which bacterial reduction of sulfates to sulfides would have been crucial for mineralization. Pb isotope studies suggest a model age of 1.8 ± 0.04 Ga for the Rampura Agucha deposit (Deb *et al.* 1989). At 1.5 Ga, the lower crustal rocks of the BGC were thrust over the western margin of the Bhilwara Supergroup, resulting in upper amphibolite facies metamorphism (Deb *et al.* 1989, Deb & Sarkar 1990, Sugden *et al.* 1990) in the Rampura Agucha area.

The results reported herein form part of an ongoing geoscientific investigation directed toward a characterization of mineralogy, geochemistry and genesis of the Rampura Agucha deposit. This work is being carried

out by staff of the Institute of Geological Sciences, Mining University, Leoben, Austria, in collaboration with Hindustan Zinc Ltd. The aim of this paper is to report the results of a detailed study of the ore minerals, their distribution and chemistry within the Rampura Agucha deposit, in order to enhance recovery of these metals during ore extraction and concentration. A study of the textures and the relation of the ore minerals to metamorphism is another important part of this paper.

Geological Setting and Orebody

The deposit occurs in a doubly plunging synformal structure of elliptical shape, comprising sillimanite- and graphite-bearing mica schist enclosed in garnet – biotite – sillimanite gneiss, with minor bands of amphibolite and calc-silicate rocks, as well as aplite, granitic pegmatite and mylonite. The orebody, hosted by a graphite – mica – sillimanite schist, is lens-shaped, with a northeast–southwest strike length of 1600 m and a width varying from a few meters in the northeast to as much as 100 m in the central and southwest section (Fig. 2). The orebody dips between 50 and 80° (average dip of approximately 60°) southeast and has been proved by drilling to a depth of 370 m from the surface (Gandhi *et al.* 1984). The semimassive orebody exhibits sharp contacts with the footwall and the hanging-wall rocks. No major faults have been detected in the orebody, although minor faults have been traced in some segments of the ore zone (Gandhi *et al.* 1984). The deposit has an oxidized gossan and a small zone of partially oxidized material between gossan and protore. Since the greater part of the area is capped with soil cover, and fresh outcrops are scarce, much of the detailed geological information was obtained from drill cores.

The mineralization occurs predominantly as disseminations in a schist, consisting of quartz, feldspar (alkali feldspar and plagioclase), sillimanite, graphite and various micaceous minerals (muscovite, biotite and chlorite). Sphalerite, by far the most widespread sulfide mineral, occurs with galena, pyrite and pyrrhotite in varying proportions, with numerous inclusions of rounded to subrounded grains of feldspar and quartz. Graphite, a common gangue mineral, represents 6 to 10 vol.% of the bulk of average ore. A large variety of minor sulfide phases occurs within the ore, the most important being pyrargyrite, freibergite and Ag–(Pb)–Sb sulfosalts. Ore microscopy of samples from 20 drill-core intersections did not reveal any zonation of those metals within the orebody, although the Zn:Pb:Fe proportions vary within meters. Although sphalerite is the most important base-metal sulfide at Rampura Agucha, small sections of the orebody can be dominated by either galena or pyrrhotite. Peak metamorphic conditions of upper amphibolite to granulite facies were estimated by garnet–hornblende and garnet–biotite thermometry (650–700°C), sphalerite barometry and fluid-inclusion studies (~6 kbar) (Ranawat *et al.* 1988, Deb 1992). The metamorphism

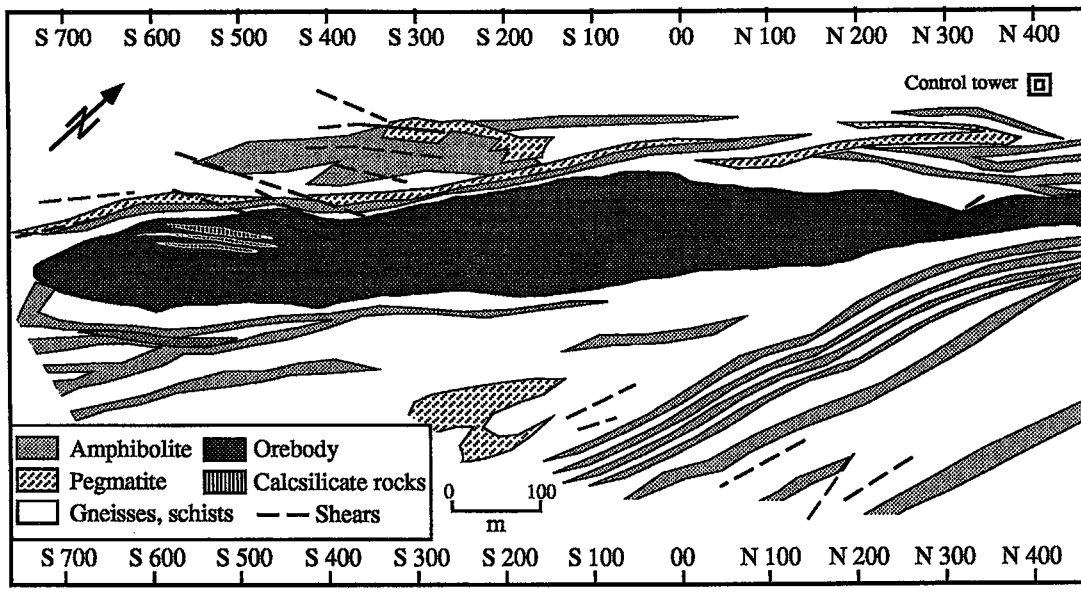

Fig. 2. Simplified geological map of Rampura Agucha orebody and surrounding rocks.

was isochemical, but led to a redistribution of the sulfide minerals within the orebody. High-grade peak metamorphism was followed by a clockwise retrograde P–T cooling path. The deposit also underwent polyphase deformation (Ray 1980). The high-grade metamorphic event resulted in a high degree of recrystallization (aggregates of sulfides with grain sizes exceeding 3 mm) and an obliteration of most of the primary sedimentary textures. Primary mineral banding is very rare, but can be observed in a few polished sections, indicating a synsedimentary origin. Remobilization of galena and sphalerite and, to a lesser degree, of pyrrhotite is common; quartz and feldspar, which are highly deformed, exibit numerous cracks, filled with sulfides and sulfosalts. Sandwich-like intergrowths of sulfides with graphite and phyllosilicates are very common. The characteristic ball texture described by Ranawat *et al.* (1988), consisting of rolled porphyroclasts of silicates and sulfides, has been observed in several samples. Oxide minerals (rare Cr–V oxides, gahnite and pyrophanite) were formed by interaction of silicate and sulfide minerals as a consequence of high-grade metamorphism (Höller & Stumpfl 1995).

Methods of Investigation

Detailed ore petrography of 97 drill-core chip samples from across the strike length and depth of the orebody has been documented to investigate metal zoning in the orebody and Ag-zoning in tetrahedrite–tennantite-group minerals, and simply to establish the identity of the Ag minerals. The sulfides were analyzed with an ARL–SEMQ electron microprobe (wavelength-dispersion spectrometry) at the Institute of Geological Sciences, Leoben, using matrix corrections according to the procedures of Bence & Albee (1968). Acceleration voltage used for sulfide analysis was generally 15 kV, and for Pb-bearing phases, 25 kV, with a beam current of 20 nA. Pure metals (Ag, Cd, Co), alloys (SeCu) and natural chalcopyrite (Fe, Cu, S), sphalerite (Zn), galena (Pb), bismuthinite (Bi), and breithauptite (Ni) were used as standards for the analysis of sulfides and sulfosalts.

Sulfides, Graphite and Sulfosalts

Sphalerite, which is the predominant sulfide mineral, occurs as coarse- to fine-grained aggregates in

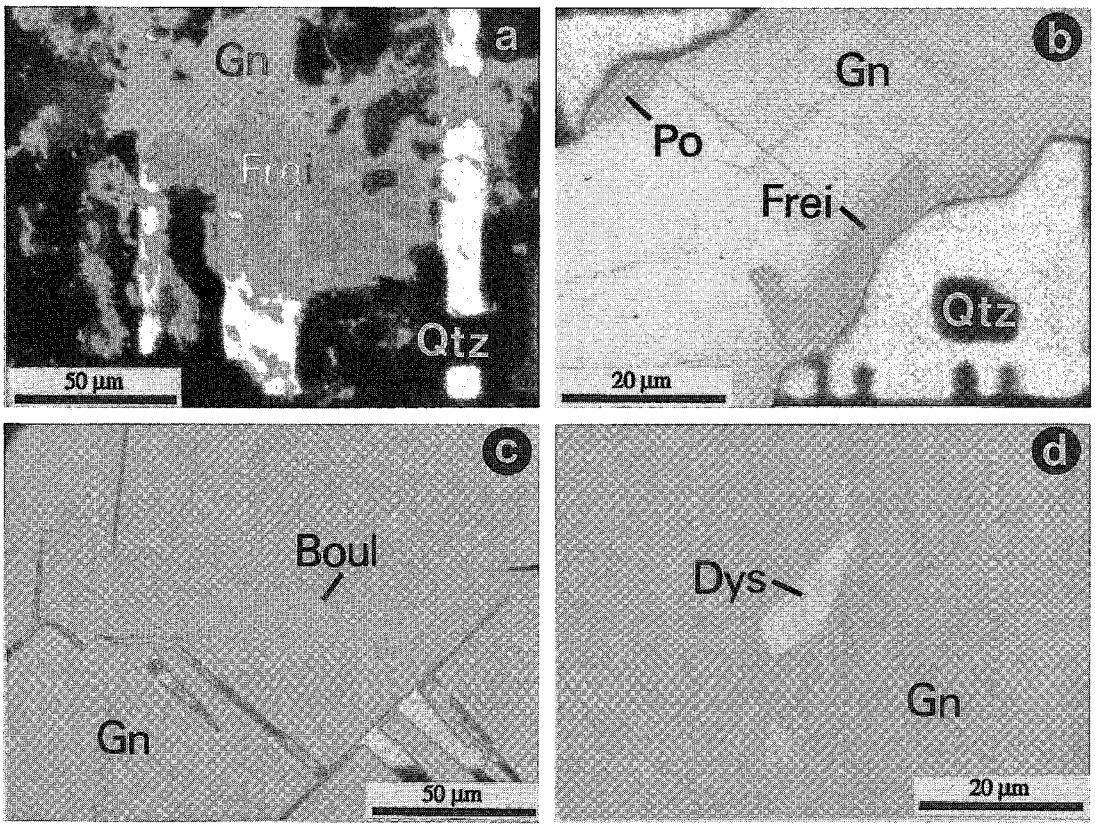

close association with galena, pyrrhotite and pyrite. The coarse-grained variety locally retains evidence of metamorphic recrystallization: characteristic 120° triple-point grain junctions and homogeneous Fe contents (up to 11.5% Fe, 0.5% Mn, 0.3% Cd). A small grain of sphalerite (15 μm across) with inclusions of chalcopyrite contains considerable amounts of Cd (up to 9 %) and Mn (up to 10%). Aggregates of sphalerite commonly contain inclusions of galena and graphite, as well as exsolved blebs of pyrrhotite.

Galena occurs as coarse-grained aggregates in close association with sphalerite and pyrrhotite, or encloses subrounded gangue minerals and other sulfides. Remobilization of galena along fissures and cleavages of gangue minerals is widespread. The concentration of minor constituents, such as Bi, Sb, Ag and Se, is below the detection limit of the electron microprobe.

Pyrite forms granular aggregates of polygonal crystals (up to 5 mm across), but may be intergrown with pyrrhotite and marcasite. Large porphyroblasts of pyrite show brittle fractures filled with other sulfide minerals. Porphyroblasts of pyrite within cataclastic sphalerite indicate the formation of at least some of the pyrite after cataclasis.

Pyrrhotite generally forms coarse aggregates of polygonal grains, displaying metamorphic crystallization. It occurs as fine-grained aggregates intergrown with other sulfides or as exsolved inclusions in sphalerite. Pyrrhotite grains are often incipiently (or completely) decomposed to a granular product,

FIG. 3. Modes of occurrence of Ag-rich minerals under reflected light in oil immersion. (a) Anhedral freibergite (Frei) in remobilized galena (Gn). (b) Subhedral grain of freibergite in galena at the grain contact with quartz (Qtz). Adjacent grain is pyrrhotite (Po). (c) Flakes of boulangerite (Boul) in galena. (d) Subhedral to euhedral exsolution-induced bodies of dyscrasite (Dys) in galena. (e) Pyrargyrite (Pya) intergrown with chalcopyrite (Ccp) and remnants of pyrite (Py), probably occurring as a pseudomorph after freibergite and pyrite and rimmed by galena (Gn) and biotite (Bt). (f) Complex intergrowth of Pb–Ag–Sb sulfosalt (light grey, arrows) with surrounding pyrargyrite and boulangerite in galena. (g) Complex intergrowth of argentite (Arg) and pyrargyrite (Pya) relics in stephanite (Stp) adjacent to pyrite (Py, poorly polished). Sulfosalt to the right is pure stephanite, rimmed by galena and quartz (Qtz). (h) Intergrowth of gudmundite (Gud), chalcopyrite (Ccp) and sphalerite (Sp), rimmed by galena and plagioclase (Pl).

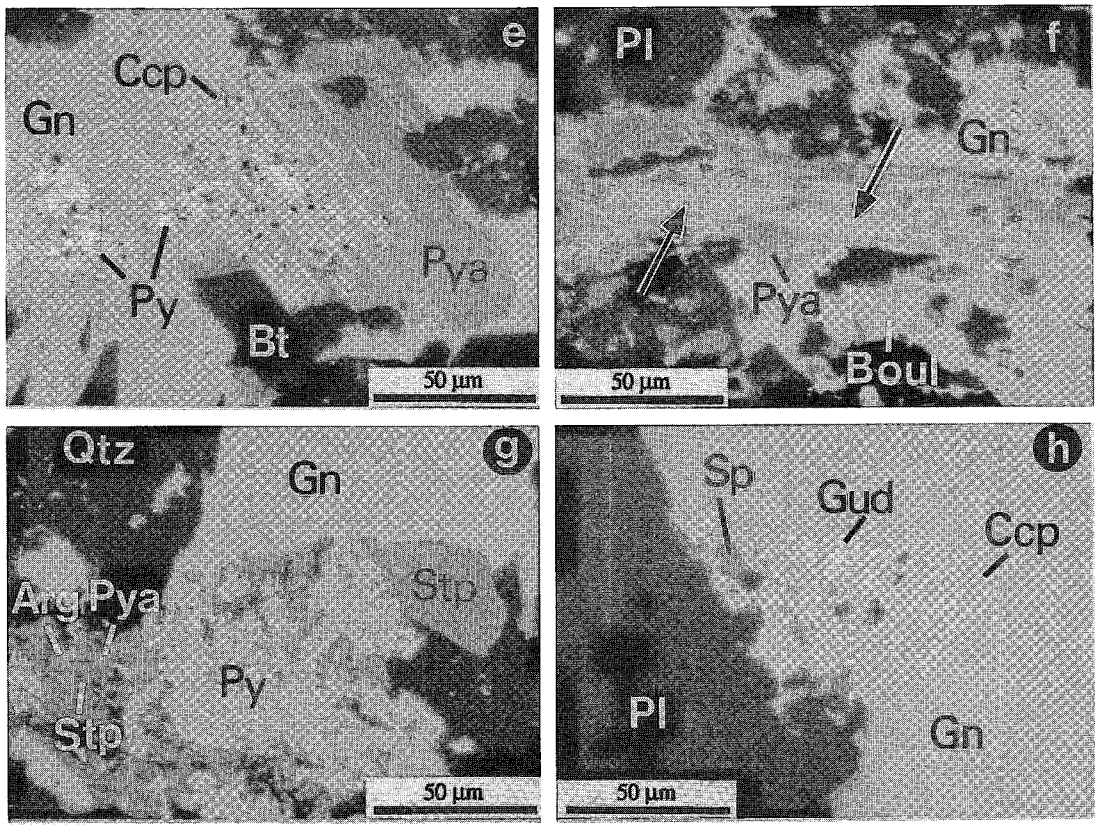

consisting of pyrite and marcasite. Pyrrhotite is invariably relatively pure, containing no more than traces of Co and Ni.

Graphite is a common gangue mineral in all samples of the graphite – mica – sillimanite schist. It occurs as flakes (0.01–3 mm across), or as fracture fillings and along grain boundaries. Graphite also encloses other ore and gangue minerals, and occurs as small inclusions in quartz, feldspar and the ore minerals. Folded graphite flakes and kink bands indicate a differential stress-and-strain effect in the area.

Arsenopyrite, a common minor constituent in metamorphosed massive sulfide deposits, forms subhedral to euhedral crystals (up to 3 mm across) that are occasionally flattened parallel to the foliation in highly deformed samples. Occasionally bent crystals display evidence of plastic deformation. Large crystals may enclose a core of *löllingite* ($FeAs_2$). The arsenopyrite contains up to 0.5% Ni and 0.45% Co, and the löllingite carries up to 3% Ni, 0.55% Co and 2.5% S. *Chalcopyrite* has been found as a minor constituent (up to 100 μm across) and occurs as disseminated anhedral grains interstitial to the dominant iron sulfides and silicates. It is also intergrown with either pyrargyrite or gudmundite (Figs. 3e, h). *Gudmundite* (FeSbS), *breithauptite* (NiSb), *ullmannite* (NiSbS) and *native antimony* occur as compact inclusions in aggregates of massive galena, or form irregular intergrowths in remobilized veinlets with galena and pyrargyrite. A complex intergrowth of gudmundite and chalcopyrite has been observed at the margin of large grains of galena (Fig. 3h). The gudmundite contains up to 0.5% Zn, 0.2% Ag and 0.6% Ni; the ullmannite carries up to 0.3% Fe and 0.4% Ag. *Greenockite* (CdS) forms anhedral grains (<20 μm across) within galena and commonly is associated with boulangerite and freibergite. It contains up to 1.2% Mn, 1.4% Fe and 0.9% Zn. *Molybdenite* either occurs as anhedral grains (<30 μm across) in close association with galena, or forms flakes and fracture fillings in sphalerite. A thallium-bearing mineral with the idealized formula $(Cu,Ag,Tl)FeS_2$ occurs as inclusions in galena. It was first described by Genkin & Schmidt (1991).

Freibergite $(Ag,Cu,Fe,Zn)_{12}(Sb,As)_4S_{13}$ is an abundant phase in Ag-rich samples. It occurs as inclusion-free anhedral grains (5–50 μm across), usually at the margin of coarse aggregates of galena grains close to contacts with silicates (Fig. 3b) or other sulfides, or is invariably included within remobilized galena (Fig. 3a). In reflected light, its color varies from olive-green to grey-green, without correlation to the extent of Ag-for-Cu substitution. Electron-microprobe analyses were carried out on forty-six grains of freibergite from ten samples. In this deposit, single grains of freibergite are chemically homogeneous, and no marked compositional changes were detected across individual grains, although different grains of the same sample may vary. The Ag-content of most grains ranges from 28 to 36%, with a maximum around 31%; the Cu-content ranges from 10 to 18%, with a maximum around 15% (Table 1). The lowest Cu-contents correspond to the highest Ag-contents, suggesting a Ag-for-Cu substitution (Fig. 4). Three grains of freibergite show lower Ag-contents (17–20%), and two grains show higher Ag-contents (38 and 41%). Despite these differences in Ag-content, these grains show the same textural criteria and color as grains with common Ag and Cu contents (around 31% Ag) in the same sample. There is no correlation between the contents of Fe (4.1–8.3%), Zn (0–2.1%), As (0–1.6%), and Ag or Cu. At Agucha, the freibergite is similar in composition to freibergite from Mount Isa (Riley 1974). A study of freibergite from several profiles through the entire orebody, from footwall to hanging wall, did not reveal any Cu-for-Ag zoning.

TABLE 1. CHEMICAL COMPOSITION OF SILVER-BEARING MINERALS FROM THE RAMPURA AGUCHA DEPOSIT AND OF FREIBERGITE FROM MT. ISA

	Arg	Stp 1	Stp 2	Pya 1	Pya 2	Frei 1	Frei 2	Frei 3	Mt.Isa
S	14.88	14.88	15.86	17.88	16.67	21.44	19.92	19.58	20.40
Fe	0.40	0.60	0.89	0.05	0.47	5.16	5.24	4.97	5.40
Ag	82.42	69.76	67.29	59.23	60.16	30.58	34.50	37.76	33.20
Sb	2.57	14.61	15.08	21.64	22.33	25.19	25.83	25.40	25.40
As	0.05	0.36	1.01	0.79	0.65	1.39	0.82	0.70	0.40
Cu	0.50	-	0.51	-	0.25	14.95	13.28	10.86	13.30
Zn	-	-	-	-	-	1.12	0.61	0.23	1.00
Pb	-	-	-	0.20	0.22	-	-	0.34	-
Σwt.%	100.82	100.21	100.64	99.79	100.75	99.83	100.20	99.84	99.10
S	1.00	3.73	3.86	3.01	2.85	12.73	12.26	12.27	12.52
Fe	0.02	0.09	0.13	-	0.04	1.76	1.86	1.79	1.89
Ag	1.91	5.18	4.87	2.97	3.04	5.40	6.30	7.03	6.02
Sb	0.05	0.96	0.97	0.96	1.01	3.93	4.18	4.18	4.08
As	-	0.04	0.10	0.06	0.04	0.36	0.20	0.18	0.10
Cu	0.02	-	0.06	-	0.02	4.49	4.00	3.44	4.10
Zn	-	-	0.01	-	-	0.33	0.20	0.08	0.29
Pb	-	-	-	-	-	-	-	0.03	-
Σ	3.00	10.00	10.00	10.00	7.00	29.00	29.00	29.00	29.00

	Dys 1	Dys 2	Sulfo 1	Sulfo 2	Sulfo 3	Sulfo 4	Boul 1	Boul 2	My
S	1.12	-	16.32	18.14	16.70	17.46	18.62	17.82	21.55
Fe	-	-	-	0.24	-	-	-	0.10	0.09
Ag	69.06	77.24	43.32	28.61	19.86	12.65	-	2.24	35.80
Sb	26.08	22.10	21.68	30.75	21.64	23.92	25.69	24.53	42.48
As	1.00	-	0.61	0.77	0.49	0.40	0.27	0.10	0.25
Pb	1.06	-	17.33	22.06	40.50	45.39	55.20	54.28	-
Σwt.%	98.32	99.34	99.26	100.57	99.19	99.82	99.78	99.07	100.17
S	0.15	-	6.91	7.52	7.68	8.05	10.98	10.71	1.99
Fe	-	-	-	0.05	-	-	-	-	-
Ag	2.83	3.19	5.43	3.52	2.71	1.73	-	0.40	0.98
Sb	0.94	0.81	2.41	3.36	2.62	2.91	3.99	3.86	1.02
As	0.06	-	0.11	0.13	0.10	0.07	-	-	0.01
Pb	0.02	-	1.14	1.42	2.89	3.24	5.03	5.03	-
Σ	4.00	4.00	16.00	16.00	16.00	16.00	20.00	20.00	4.00

Symbols: Arg: argentite, Stp: stephanite, Pya: pyrargyrite, Frei: freibergite, Dys: dyscrasite, Sulfo: Pb–Ag–Sb sulfosalt, Boul: boulangerite, My: myargyrite. Data on freibergite from Mt. Isa are taken from Riley (1974).

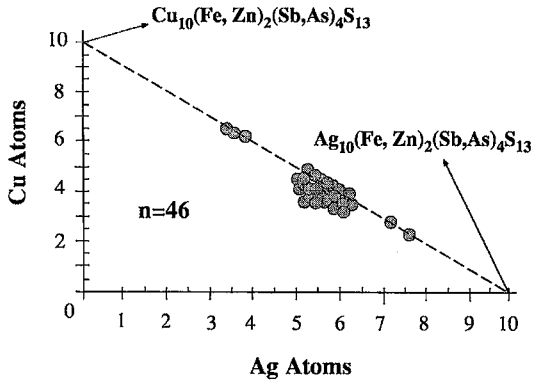

FIG. 4. Variation of Ag and Cu in freibergite from Rampura Agucha, calculated on the basis of 29 atoms.

Pyrargyrite (Ag_3SbS_3) is the predominant Ag-bearing phase of the Agucha orebody. It commonly occurs as anhedral, disseminated grains (5–35 μm across) in veinlets together with remobilized galena, chalcopyrite and Sb-minerals. It also forms complex intergrowths with (or a narrow rim around) Ag–Pb–Sb sulfosalts (Fig. 3f). Pyrargyrite also occurs in close association with pyrite and pyrrhotite, where it forms larger subhedral to euhedral grains (up to 100 μm across), and it tends to be associated with chalcopyrite (Fig. 3e). Individual grains are chemically homogeneous; although arsenopyrite is present in the same ore zones, As-contents do not exceed 1% (Table 1).

Ag–Pb–Sb sulfosalts are common but not as widespread as pyrargyrite and freibergite. They are located invariably in the interior of large aggregates of galena, where they typically occur as anhedral inclusions

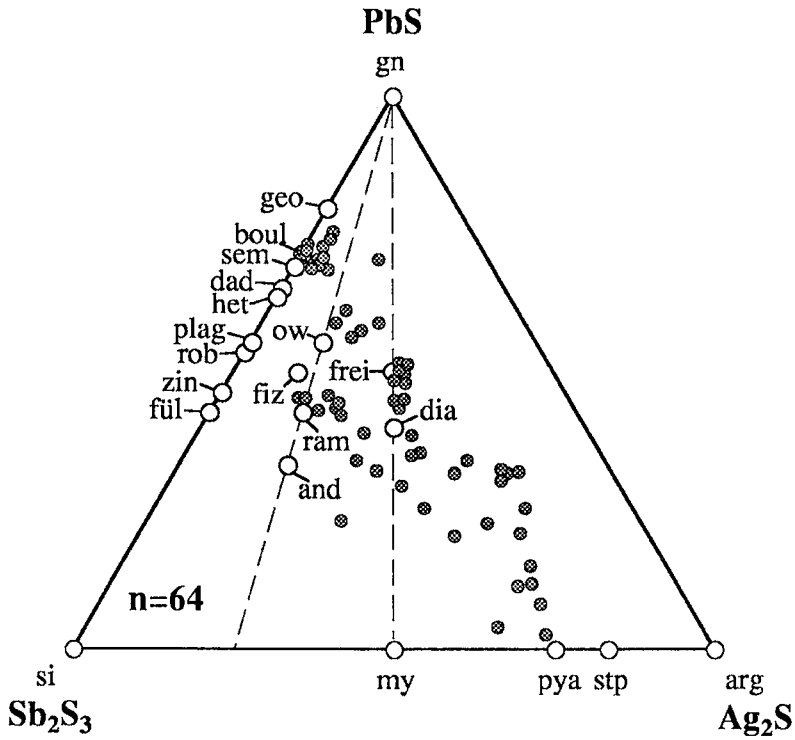

FIG. 5. Compositional variation of Pb–Ag sulfosalts from the Rampura Agucha deposit (•) in the ternary system Sb_2S_3–PbS–Ag_2S_3. Additional end-member minerals (○) are derived from Craig *et al.* (1973), Goodell (1975) and Keighin & Honea (1969). Ideal compositions, symbols and formulas of the known sulfosalts and sulfides are shown: gn: galena, PbS; geo: geocronite, $27PbS{\cdot}7Sb_2S_3$; boul: boulangerite, $5PbS{\cdot}2Sb_2S_3$; sem: semseyite, $9PbS{\cdot}4Sb_2S_3$; het: heteromorphite, $7PbS{\cdot}4Sb_2S_3$; plag: plagionite, $5PbS{\cdot}4Sb_2S_3$; rob: robinsonite, $7PbS{\cdot}6Sb_2S_3$; zin: zinckenite, $6PbS{\cdot}7Sb_2S_3$; fül: füllöppite, $3PbS{\cdot}4Sb_2S_3$; dad: dadsonite, $11PbS{\cdot}6Sb_2S_3$; ow: owyheeite, $5PbS{\cdot}3Sb_2S_3{\cdot}Ag_2S$; fiz: fizelyite, $5PbS{\cdot}4Sb_2S_3{\cdot}Ag_2S$; ram: ramdohrite, $3PbS{\cdot}3Sb_2S_3{\cdot}Ag_2S$; frei: freieslebenite, $2PbS{\cdot}Sb_2S_3{\cdot}Ag_2S$; dia: diaphorite, $4PbS{\cdot}3Sb_2S_3{\cdot}Ag_2S$; and: andorite, $2PbS{\cdot}Sb_2S_3{\cdot}Ag_2S$; si: stibnite, Sb_2S_3; my: miargyrite, $Sb_2S_3{\cdot}Ag_2S$; pya: pyrargyrite, $Sb_2S_3{\cdot}3Ag_2S$; stp: stephanite, $Sb_2S_3{\cdot}5Ag_2S$; arg: argentite, Ag_2S.

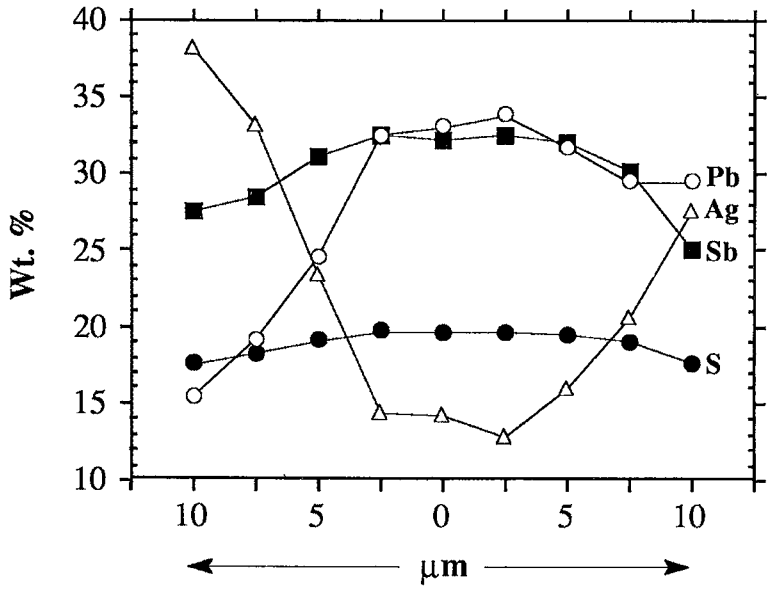

FIG. 6. Traverse across a zoned grain of Ag–Pb–Sb sulfosalt.

(10–25 μm across). Occasionally complex intergrowths with pyrargyrite (Fig. 3f) occur within large aggregates of galena. Their color in reflected light resembles that of galena, but the reflectivity is slightly lower. The Ag–Pb–Sb sulfosalts are strongly anisotropic and lack internal reflections. Microprobe analyses reveal considerable compositional variations (Fig. 5, Table 1). A few grains are significantly zoned (Fig. 6). Seven data points encountered (Fig. 5) plot near the idealized composition of *freieslebenite* ($AgPbSbS_3$).

Boulangerite ($Pb_5Sb_4S_{11}$) forms flakes (10–50 μm across) in galena (Fig. 3c) and is commonly encountered in complex intergrowths with Ag–Pb–Sb sulfosalts and pyrargyrite (Fig. 3f). Although most aggregates are devoid of Ag, some grains contain up to 2% Ag (Fig. 5, Table 1). *Dyscrasite* (Ag_3Sb) forms tiny, single-phase subhedral to euhedral grains (<10 μm across) that are characteristically disseminated in the interior of large aggregates of galena (Fig. 3d). It is not found in contact with other Ag minerals. Low contents of Pb, Sb and S have been determined (Table 1). *Stephanite* (Ag_5SbS_4) (5–50 μm across) is found in a few Ag-rich samples and occurs in close association with galena, pyrargyrite and pyrite (Fig. 3g). Minor contents of As and Cu have been detected (Table 1). *Argentite* (Ag_2S) is rare and forms tiny anhedral grains (<5 μm) in close association with pyrargyrite and stephanite (Fig. 3g). *Polybasite* $(Ag, Cu)_{16}Sb_2S_{11}$ (Mukherjee *et al.* 1991) and *miargyrite* $AgSbS_2$ also are rare and occur as vein minerals in sphalerite. Miargyrite contains up to 0.4% As, and all other trace elements are below the detection limit.

DISCUSSION

The regional metamorphic history (Ranawat & Sharma 1990, Deb *et al.* 1989) includes a high-grade event with peak conditions of 650–700°C and ~6 kbar in the Rampura Agucha area, and it affected the stratiform orebody. The high-grade metamorphism was almost isochemical on a large scale, although a number of components have been redistributed locally during metamorphism and retrogression. It is difficult to determine which features in the ore relate to the prograde event and which reflect retrograde equilibration. The high-grade metamorphic event resulted in thorough recrystallization of most sulfides, development of triple-point junctions, ductile deformation of pyrite and arsenopyrite, the development of porphyroblasts and the formation of characteristic metamorphic minerals such as sillimanite and gahnite. Primary sulfide minerals were homogenized, so that original compositional zoning, if ever present, is no longer observable. Only Ag–Pb–Sb sulfosalts, which seem to have formed during the waning stage of the metamorphic event, may be zoned (Fig. 6). The ore minerals seem to have behaved differentially during metamorphism. Pyrite, pyrrhotite and sphalerite tend to maintain a constant shape, whereas galena, which was by far the most mobile sulfide, almost everywhere exhibits evidence of plastic deformation and remobilization. To a lesser extent, sphalerite and pyrrhotite were remobilized into the silicate minerals during and after high-grade metamorphism. All sulfide minerals except pyrite commonly fill fractures in quartz, feldspar, and mica; there, stephanite, freibergite and

pyrargyrite may be minor constituents.

Galena-rich samples from the Rampura Agucha orebody contain eight defined Ag-bearing ore minerals and a number of intermediate compositions in the ternary system $PbS–Ag_2S–Sb_2S_3$. Sphalerite-dominated samples tend to be devoid of any Ag-bearing minerals. Pyrargyrite, freibergite and Ag–Pb–Sb sulfosalts represent the most widespread Ag-minerals. Stephanite, argentite, miargyrite, dyscrasite and polybasite are less common. Sulfosalts are highly susceptible to retrogression and generally undergo continual re-equilibration to low temperatures (Vaughan & Craig 1978). Freibergite, boulangerite and argentite are most probably prograde sulfosalts at Rampura Agucha, present at the peak of metamorphism. The upper limits of stability for iron-rich tetrahedrite (6.9 at.% Fe) and S-rich argentite are 661°C in the system Cu–Fe–Sb–S (Tatsuka & Morimoto 1977) and 622°C in the system Ag–Sb–S (Keighin & Honea 1969), respectively. At higher temperatures, these minerals melt. Boulangerite has an upper stability limit of 637°C in the system Pb–Sb–S (Salanci 1979). The limited solubility of Sb_2S_3 in galena (3 mol% at 640°C; Salanci 1979) would also suggest the appearance of a separate Sb_2S_3-bearing phase at this stage. However, interpretation of these stability limits could be ambiguous. The stability curves are pressure-dependent, in the order of 6–10°C per kbar or less in the system Pb–Sb–S (Garvin 1973), and additional elements such as Zn or As also may result in a shift of the stability curves (Craig & Kullerud 1968, Tatsuka & Morimoto 1973, 1977). Pyrargyrite, the most common Ag-mineral, has an upper stability limit of 485°C in the system Ag–Sb–S (Keighin & Honea 1969) and thus formed during the retrograde part of the P–T path. Although there is no direct evidence for a breakdown of freibergite, the occurrence of gudmundite, chalcopyrite and sphalerite grains (Fig. 3h), as well as pyrargyrite–chalcopyrite intergrowths that form large, subhedral pseudomorphs (presumably after freibergite) in galena (Fig. 3e), suggests that the following retrograde reactions took place (not balanced):

$$\underset{\text{tetrahedrite}}{(Cu,Fe,Zn)_{12}Sb_4S_{13}} + \underset{\text{pyrite}}{FeS_2} \rightarrow \underset{\text{chalcopyrite}}{CuFeS_2} + \underset{\text{gudmundite}}{FeSbS} + \underset{\text{sphalerite}}{ZnS} \quad (1)$$

$$\underset{\text{freibergite}}{(Ag,Cu,Fe,Zn)_{12}Sb_4S_{13}} + \underset{\text{pyrite}}{FeS_2} \rightarrow \underset{\text{chalcopyrite}}{CuFeS_2} + \underset{\text{pyrargyrite}}{Ag_3SbS_3} \pm \underset{\text{sphalerite}}{ZnS} \quad (2)$$

It has been demonstrated at several metamorphosed deposits that freibergite, tennantite and tetrahedrite break down during cooling. At Broken Hill, New South Wales (Plimer 1980, Both & Stumpfl 1987), tetrahedrite reacts to chalcopyrite and gudmundite. At Rajpura Dariba, Rajasthan (Kanika Basu *et al.* 1984) and Cofer, Virginia (Miller & Craig 1983), the tetrahedrite–tennantite-group mineral decomposes to arsenopyrite, chalcopyrite, gudmundite and sphalerite. At Långdal, Sweden (Karup-Møller *et al.* 1989), freibergite has reacted to pyrargyrite and chalcopyrite. An upper stability limit of gudmundite of 280 ± 10°C in the system Fe–Sb–S (Clark 1966) indicates that reaction (1) took place at the end of the retrograde stage of the metamorphic evolution.

Pyrargyrite and stephanite may also have formed by a breakdown of Ag–Pb–Sb sulfosalts. Replacement of Ag–Pb–Sb sulfosalts (presumably freieslebenite; Fig. 3f) by pyrargyrite and boulangerite in galena suggests the following retrograde reaction:

$$\underset{\text{Ag–Pb–Sb sulfosalt}}{Ag_3Pb_{3.2}Sb_{2.9}S_{8.6}} \rightarrow \underset{\text{pyrargyrite}}{Ag_3SbS_3} + \underset{\text{galena}}{PbS} + 0.45\ \underset{\text{boulangerite}}{Pb_5Sb_4S_{11}} \quad (3)$$

A similar reaction is reported from other localities: for example, at Tetyuhke, Russia, andorite is replaced by pyrargyrite, owyheeite and stephanite (Natarov *et al.* 1972); at Rivertree, New South Wales, owyheeite is replaced by pyrargyrite and galena (Lawrence 1962); at the Meerschaum mine, Mt. Wills, Victoria, andorite is replaced by miargyrite and owyheeite (Birch 1981), and at Morea, Nevada, andorite is replaced by diaphorite, diaphorite by owyheeite, and owyheeite by galena and pyrargyrite (Williams 1968). Alhough some compositions of Ag–Pb–Sb sulfosalts from Agucha plot close to the idealized composition of freieslebenite ($AgPbSbS_3$), most display intermediate compositions between the end-member minerals. A few grains are zoned, and no obvious trend in zoning patterns was observed, although an influence of retrograde metamorphism on the zonation of Ag–Pb–Sb sulfosalts cannot be ruled out. Hoffman & Trdlicka (1978) compared compositions of owyheeite ($Ag_2Pb_5Sb_6S_{15}$) from seven deposits, and showed that the chemical compositions are highly variable (40.77–46.45 wt.% Pb). Moëlo *et al.* (1984) showed that substitution of the major cations (mainly $2\ Pb^{2+} \leftrightarrow Ag^+ + Sb^{3+}$) is responsible for the significant variation in the composition of owyheeite from thirteen ore deposits. The lowest Ag-contents of some zoned Ag–Pb–Sb sulfosalts from the Agucha deposit correspond to the highest Pb- and Sb-contents, suggesting mainly a Ag-for-(Pb+Sb) substitution (Fig. 6).

Stephanite, a relatively common retrograde mineral, is found in small amounts in many Ag-deposits. It is a typical secondary mineral phase that formed from other Ag-sulfosalts. Stephanite has an upper stability limit of 197 ± 5°C in the system Ag–Sb–S (Keighin & Honea 1969), indicating formation at the end of the retrograde metamorphic path. Relics of argentite and pyrargyrite in stephanite grains (Fig. 3g) indicate the following

retrograde reaction:

$$\underset{\text{argentite}}{Ag_2S} + \underset{\text{pyrargyrite}}{Ag_3SbS_3} \rightarrow \underset{\text{stephanite}}{Ag_5SbS_4} \quad (4)$$

The formation of stephanite at the expense of pyrargyrite and argentite is also reported from Garpenberg Norra, central Sweden (Sandecki 1983).

Dyscrasite, a common Ag-bearing inclusion in galena (Sharp & Buseck 1993) forms tiny inclusions (<20 μm, Fig. 3d) uniformly distributed in the interior of large aggregates of galena (>3 mm). These types of inclusions have been interpreted as due to exsolution of an Ag–Sb rich phase from galena, attributed to a decreasing solubility of these elements in galena at lower temperatures. On the basis of their experimental work, Hall & Czamanske (1972) and Sandecki & Amcoff (1981) suggested the formation of Ag–Sb phases by exsolution from galena between 350 and 400°C.

Conclusions

This study of Ag-bearing sulfosalts has established the mineral composition and paragenesis of freibergite, pyrargyrite, stephanite, dyscrasite, various Ag–(Pb)–Sb sulfosalts and several minor important Ag minerals from the Agucha deposit. The present Ag-mineralogy reflects the metamorphic evolution of this stratiform deposit. The premetamorphic Ag-minerals, present at the time of formation of the deposit, remain unknown owing to the event of high-grade metamorphism that transformed both the silicate and sulfide assemblages. Freibergite, as well as argentite, which were apparently present at the peak of metamorphism, were partially consumed during retrogression. As a result, a low-temperature assemblage comprising pyrargyrite, stephanite, gudmundite and chalcopyrite formed in close association with galena. Pyrargyrite also formed by decomposition of Ag–Pb–Sb sulfosalts. Dyscrasite exsolved from galena owing to retrograde cooling and decompression.

Acknowledgements

We thank Hindustan Zinc Ltd. for providing drill-core samples for this study, and Helmut Mühlhans for assistance with the electron-microprobe analyses. I am grateful to B. McElduff, who performed previous work on the sulfosalt assemblage, as well as R.T.M. Dobbe, of the Free University, Amsterdam, and E.F. Stumpfl, F. Melcher and J. Raith, Mining University Leoben, for helpful discussions. The constructive criticism of two reviewers as well as financial support of the Austrian Research Council (FWF) through grant No. 10322–TEC to E.F. Stumpfl are gratefully acknowledged.

References

Bence, A.E. & Albee, A.L. (1968): Empirical correction factors for the electron microprobe analysis of silicates and oxides. *J. Geol.* **76**, 382-403.

Birch, W.D. (1981): Silver sulphosalts from the Meerschaum mine, Mt. Wills, Victoria, Australia. *Mineral. Mag.* **44**, 73-78.

Both, R.A. & Stumpfl, E.F. (1987): Distribution of silver in the Broken Hill orebody. *Econ. Geol.* **82**, 1037-1043.

Clark, A.H. (1966): Heating experiments on gudmundite. *Mineral. Mag.* **35**, 1123-1125.

Craig, J.R. & Kullerud, G. (1968): Phase relations and mineral assemblages in the copper–lead–sulfur system. *Am. Mineral.* **53**, 145-161.

_____, Chang, L.L.Y. & Rees, W.R. (1973): Investigations in the Pb–Sb–S system. *Can. Mineral.* **12**, 199-206.

Deb, M. (1992): Lithogeochemistry of rocks around Rampura Agucha massive zinc sulfide ore-body, NW India – implications for the evolution of a Proterozoic "Aulakogen". *In* Metallogeny Related to Tectonics of the Proterozoic Mobile Belts (S.C. Sarkar, ed.). Balkema, Rotterdam, The Netherlands (1-35).

_____ & Sarkar, S.C. (1990): Proterozoic tectonic evolution and metallogenesis in the Aravalli–Delhi Orogenic Complex, northwestern India. *Precamb. Res.* **46**, 115-137.

_____, Thorpe, R.I., Cumming, G.L. & Wagner, P.A. (1989): Age, source and stratigraphic implications of Pb isotope data for conformable, sediment-hosted, base metal deposits in the Proterozoic Aravalli–Delhi Orogenic belt, northwestern India. *Precamb. Res.* **43**, 1-22.

Gandhi, S.M., Paliwal, H.V. & Bhatnagar, S.N. (1984): Geology and ore reserve estimates of Rampura Agucha lead–zinc deposit, Bhilwara District. *J. Geol. Soc. India* **25**, 689-705.

Garvin, P.L. (1973): Phase relations in the Pb–Sb–S system. *Neues Jahrb. Mineral., Abh.* **118**, 235-267.

Genkin, A. & Schmidt, S.H. (1991): Preliminary data of a new thallium mineral from the lead–zinc ore deposit Agucha, India. *Neues Jahrb. Mineral., Monatsh.*, 256-258.

Goodell, P.C. (1975): Binary and ternary sulphosalt assemblages in the Cu_2S–Ag_2S–PbS–As_2S_3–Sb_2S_3–Bi_2S_3 system. *Can. Mineral.* **13**, 27-42.

Hall, W.E. & Czamanske, G.K. (1972): Mineralogy and trace element content of the Wood River lead–silver deposits, Blaine County, Idaho. *Econ. Geol.* **67**, 350-361.

HOFFMANN, V. & TRDLICKA, Z. (1978): Owyheeite from Kutná Hora – a new mineral for Czechoslovakia. *Neues Jahrb. Mineral., Monatsh.*, 45-57.

HÖLLER, W. & STUMPFL, E.F. (1995): Cr–V oxides from the Rampura Agucha Pb–Zn–(Ag) deposit, Rajasthan, India. *Can. Mineral* **33**,

HZL STAFF (1992): Rampura–Agucha mine. *Mining Mag.* **167**, 372-375.

KARUP-MØLLER, S., MAKOVICKY, E. & PILSTRÖM, G. (1989): Mineralogy of the sulfosalt zone at the Långdal deposit, Boliden district, northern Sweden. *Neues Jahrb. Mineral., Abh.* **160**, 299-327.

KANIKA BASU (SANYAL), BORTNIKOV, N.S., MISHRA, B., MOOKHERJEE, A., MOZGOVA, N.N. & TSEPIN, A.I. (1984): Significance of transformation textures in fahlores from Rajpura–Dariba polymetallic deposit, Rajasthan, India. *Neues Jahrb. Mineral., Abh.* **149**, 143-161.

KEIGHIN, C.W. & HONEA, R.M. (1969): The system Ag–Sb–S from 600°C to 200°C. *Mineral. Deposita* **4**, 153-171.

LAWRENCE, L.J. (1962): Owyheeite from Rivertree, New South Wales. *Mineral. Mag.* **33**, 315-319.

MILLER, J.W. & CRAIG, J.R. (1983): Tetrahedrite–tennantite series compositional variations in the Cofer Deposit, Mineral District, Virginia. *Am. Mineral.* **68**, 227-234.

MOËLO, Y., MOZGOVA, N., PICOT, B., BORTNIKOV, N. & VRUBLEVSKAYA, Z. (1984): Cristallochimie de l'owyheeite: nouvelles données. *Tschermaks Mineral. Petrogr. Mitt.* **32**, 271-284.

MUKHERJEE, A.D., SAMHITA GLAHIRI, & BHATTACHARYA, H.N. (1991): Silver-bearing sulphosalts from Rampura Agucha massive sulfide deposit of Rajasthan. *J. Geol. Soc. India* **37**, 132-135.

NATAROV, A.G., SVESHNIKOVA, O.L. & GALYUK, V.A. (1972): First find of andorite in the USSR. *Dokl. Akad. Nauk SSSR* **206**, 189-192 (in Russ.).

PLIMER, I.R. (1980): Hydrothermal mobilization of silver during retrograde metamorphism at Broken Hill, Australia. *Neues Jahrb. Mineral., Monatsh.*, 433-439.

RANAWAT, P.S., BHATNAGAR, S.N. & SHARMA N.K. (1988): Metamorphic character of Rampura Agucha Pb–Zn deposit, Rajasthan. *Geol. Soc. India, Mem.* **7**, 397-409.

_____ & SHARMA, N.K. (1990): Petrology and geochemistry of the Precambrian Pb–Zn deposit Rampura Agucha, India. *In* Regional Metamorphism of Ore Deposits and Genetic Implications (P.G. Spry & L.T. Bryndzia, eds.). VPS, Zeist, The Netherlands (197-227).

RAY, J.N. (1980): An evaluation of the tectonic framework of the Rampura–Agucha lead–zinc deposit, Bhilwara District, Rajasthan. *Indian Minerals* **34**, 19-21.

RILEY, J.F. (1974): The tetrahedrite–freibergite series, with reference to the Mount Isa Pb–Zn–Ag orebody. *Mineral. Deposita* **9**, 117-124.

SALANCI, B. (1979): Beiträge zum System PbS–Sb_2S_3 in Beziehung zu natürlichen Blei-Antimon-Sulfomineralien. *Neues Jahrb. Mineral., Abh.* **135**, 315-326.

SANDECKI, J. (1983): Silver-rich minerals at Garpenberg Norra, central Sweden. *Neues Jahrb. Mineral., Monatsh.*, 365-374.

_____ & AMCOFF, Ö. (1981): On the occurrence of silver-rich tetrahedrite at Garpenberg Norra, central Sweden. *Neues Jahrb. Mineral., Abh.* **141**, 324-340.

SHARP, T.G. & BUSECK, P.R. (1993): The distribution of Ag and Sb in galena: inclusions versus solid solutions. *Am. Mineral.* **78**, 85-95.

SUGDEN, T.J., DEB, M. & WINDLEY, B.F. (1990): The tectonic setting of mineralization in the Proterozoic Aravalli–Delhi orogenic belt, N.W. India. *In* Precambrian Continental Crust and its Economic Resources (S.M. Naqui, ed.). Elsevier, Amsterdam, The Netherlands (367-390).

TATSUKA, K. & MORIMOTO, N. (1973): Composition variation and polymorphism of tetrahedrite in the Cu–Sb–S system below 400°C. *Am. Mineral.* **58**, 425-434.

_____ & _____ (1977): Tetrahedrite stability relations in the Cu–Fe–Sb–S system. *Am. Mineral.* **62**, 1101-1109.

VAUGHAN, D.J. & CRAIG, J.R. (1978): *Mineral Chemistry of Metal Sulfides.* Cambridge Univ. Press, Cambridge, U.K.

WILLIAMS, S.A. (1968): Complex silver ores from Morea, Nevada. *Can. Mineral.* **9**, 478-484.

Received February 8, 1995, revised manuscript accepted June 21, 1995.